Supplement of The Cryosphere, 19, 5499–5508, 2025 https://doi.org/10.5194/tc-19-5499-2025-supplement © Author(s) 2025. CC BY 4.0 License.





Supplement of

Brief communication: Decadal changes in topography, surface water and subsurface structure across an Arctic coastal tundra site

Jonathan A. Bachman et al.

Correspondence to: Baptiste Dafflon (bdafflon@lbl.gov)

The copyright of individual parts of the supplement might differ from the article licence.

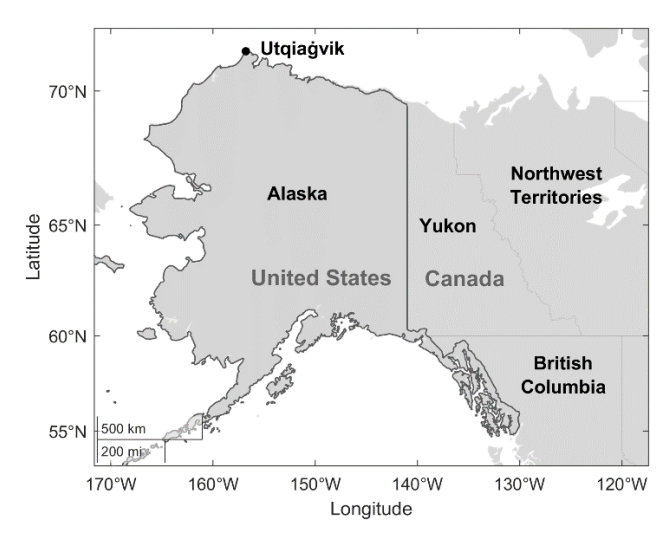


Figure S1. Geographical location of Utqiagvik, Alaska.

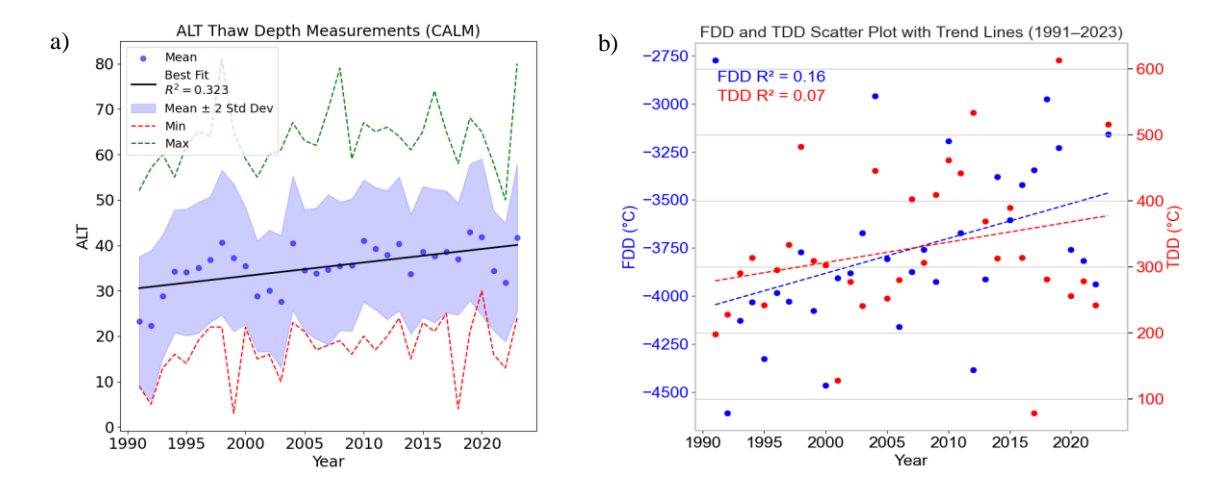


Figure S2. Temporal trends in the Utqiagvik area, including a) Active Layer Thickness (ALT) from the nearby CALM site (Shiklomanov, 2023) and b) Freezing Degree Days (FDD) and Thawing Degree Days (TDD) inferred from air temperature data from the NOAA Barrow Atmospheric Baseline Observatory. TDD was calculated by summing all positive values over the summer period, from 15 May to 31 October, and FDD by summing all negative values from 1 November to 14 May (Farquharson et al., 2022).

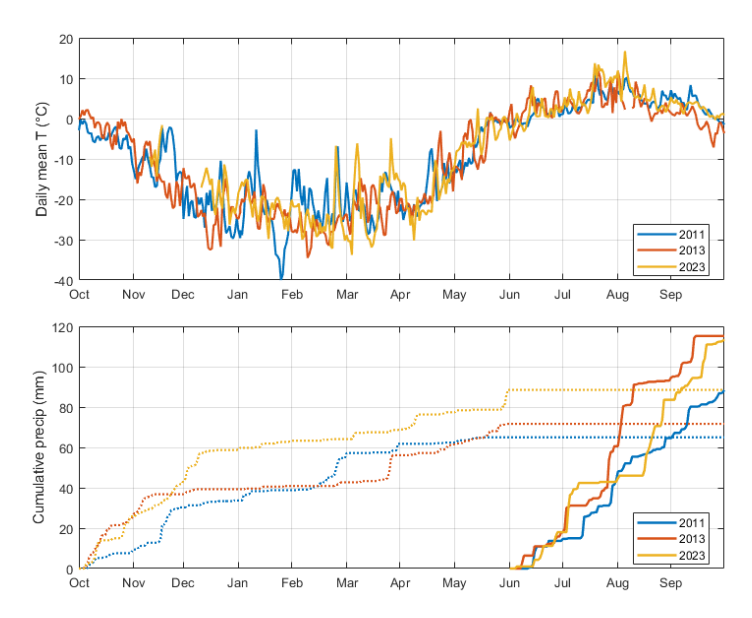


Figure S3. Air temperature (top panel) and precipitation (bottom panel) in the water year 2011, 2013 and 2023. Air temperature obtained from NOAA Barrow Atmospheric Baseline Observatory (https://gml.noaa.gov/data/data.php?category=Meteorology&site=BRW). Total precipitation obtained from Barrow Airport station (https://www.ncdc.noaa.gov/cdo-web/datasets/GHCND/stations/GHCND:USW00027502/detail), and counted as cumulative snow (dotted line) from October 1 to May 31, and cumulative rain (solid line) from June 1 to September 30.

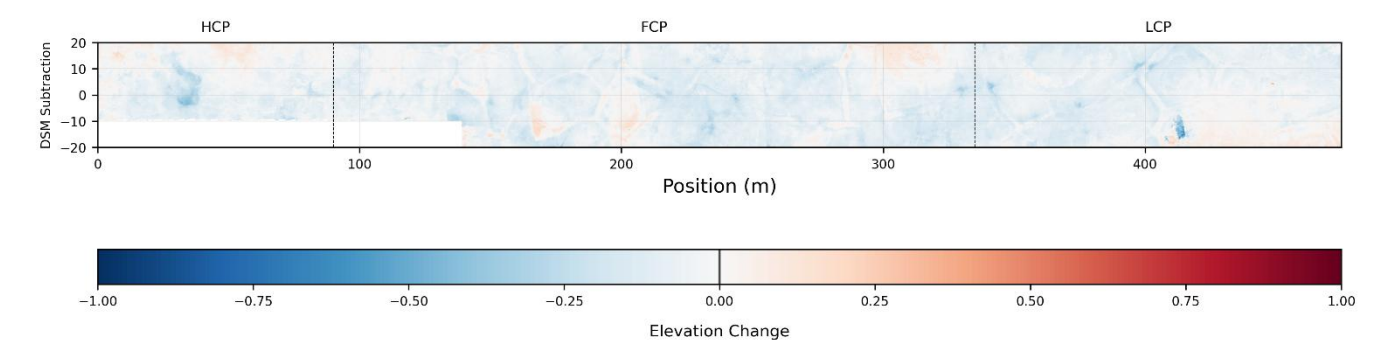


Figure S4. Difference between the digital surface models (DSMs) obtained in 2023 and 2013, with negative values indicating a decrease in elevation between 2013 and 2023. The difference along the central line, where positioning accuracy is highest due to the distribution of ground control points, is shown in Figure 1i.

Table S1: Statistical comparison between 2011 and 2023 for active layer thickness (ALT), elevation, and resistivity (R) within each polygon type (HCP = high-centered, FCP = flat-centered; LCP = low-centered). Reported are p-values from the Mann–Whitney U test (independent samples) and Wilcoxon signed-rank test (paired samples), as well as the Hodges–Lehmann estimator of the median difference with 95% confidence intervals.

Polygon type	Variable	Mann–Whitney U p-value	Wilcoxon signed- rank p-value	Hodges–Lehmann median difference	95% CI for median difference
HCP	ALT	0.049	0.0094	0.0300 m	[0.0050, 0.0550] m
FCP	ALT	< 0.001	< 0.001	0.0700 m	[0.0550, 0.0800] m
LCP	ALT	0.083	0.0060	0.0200 m	[0.0050, 0.0400] m
HCP	Elevation	< 0.001	< 0.001	-0.1026 m	[-0.1367, -0.0805] m
FCP	Elevation	< 0.001	< 0.001	-0.1041 m	[-0.1162, -0.0916] m
LCP	Elevation	< 0.001	< 0.001	-0.0738 m	[-0.0861, -0.0640] m
HCP	Log R (0-0.5m)	< 0.001	< 0.001	-0.291 log(Ohm.m)	[-0.322, -0.259] log(Ohm.m)
FCP	Log R (0-0.5m)	< 0.001	< 0.001	-0.306 log(Ohm.m)	[-0.325, -0.287] log(Ohm.m)
LCP	Log R (0-0.5m)	0.749	0.600	0.006 log(Ohm.m)	[-0.017, 0.029] log(Ohm.m)
HCP	Log R (0.5-1m)	< 0.001	< 0.001	-0.184 log(Ohm.m)	[-0.227, -0.136] log(Ohm.m)
FCP	Log R (0.5-1m)	< 0.001	< 0.001	-0.299 log(Ohm.m)	[-0.329, -0.270] log(Ohm.m)
LCP	Log R (0.5-1m)	0.316	0.228	0.02 log(Ohm.m)	[-0.012, 0.051] log(Ohm.m)
HCP	Log R (0.5-1.5m)	< 0.001	< 0.001	-0.142 log(Ohm.m)	[-0.185, -0.100] log(Ohm.m)
FCP	Log R (0.5-1.5m)	< 0.001	< 0.001	-0.290 log(Ohm.m)	[-0.320, -0.255] log(Ohm.m)
LCP	Log R (0.5-1.5m)	0.315	0.036	-0.030 log(Ohm.m)	[-0.059, -0.002] log(Ohm.m)